The AAPS Journal (2018) 20: 73
DOI: 10.1208/s12248-018-0233-6

Research Article

Theme: Pioneering Pharmaceutical Science by Emerging Investigators
Theme Editor: Ho-Leung Fung

Vaccine Adjuvant Incorporation Strategy Dictates Peptide Amphiphile Micelle Immunostimulatory Capacity

Rui Zhang,[1] Jake S. Kramer,[2] Josiah D. Smith,[1] Brittany N. Allen,[3] Caitlin N. Leeper,[1] Xiaolei Li,[1] Logan D. Morton,[1] Fabio Gallazzi,[4] and Bret D. Ulery[1,3,5]

Received 26 March 2018; accepted 14 May 2018; published online 1 June 2018

Abstract. Current vaccine research has shifted from traditional vaccines (i.e., whole-killed or live-attenuated) to subunit vaccines (i.e., protein, peptide, or DNA) as the latter is much safer due to delivering only the bioactive components necessary to produce a desirable immune response. Unfortunately, subunit vaccines are very weak immunogens requiring delivery vehicles and the addition of immunostimulatory molecules termed adjuvants to convey protective immunity. An interesting type of delivery vehicle is peptide amphiphile micelles (PAMs), unique biomaterials where the vaccine is part of the nanomaterial itself. Due to the modularity of PAMs, they can be readily modified to deliver both vaccine antigens and adjuvants within a singular construct. Through the co-delivery of a model antigenic epitope (Ovalbumin$_{319–340}$—OVA$_{BT}$) and a known molecular adjuvant (e.g., 2,3-dipalmitoyl-S-glyceryl cysteine—Pam$_2$C), greater insight into the mechanisms by which PAMs can exert immunostimulatory effects was gained. It was found that specific combinations of antigen and adjuvant can significantly alter vaccine immunogenicity both *in vitro* and *in vivo*. These results inform fundamental design rules that can be leveraged to fabricate optimal PAM-based vaccine formulations for future disease-specific applications.

KEY WORDS: Adjuvant; Co-localization; Peptide amphiphile micelles; Subunit vaccines.

INTRODUCTION

Vaccines have become a cornerstone of human health and disease prevention (1–3). Whole pathogen vaccines consisting of killed or inactivated infectious agents are the most commonly used formulations in the clinic. Despite the considerable efficacy achieved with these vaccines, they unfortunately can be associated with a number of deleterious side effects. Cases of injection site inflammation and unwanted host reactions along with storage difficulty and arduous production processes make traditional whole pathogen vaccines increasingly less appealing as novel alternatives emerge (4–15).

Within a whole pathogen vaccine, only certain components are directly targeted by the host immune response. These constituents termed antigens are most commonly peptides which lack the complexity of the entire pathogen but can facilitate a protective host response by themselves. Unfortunately, these subunit peptide vaccines have been found to be very weak immunogens since they lack the foreign immunostimulatory components found within whole pathogens which better stimulate host immune responses against the antigens. Thus, an effective delivery vehicle is required as a compensatory means for maximizing the prophylactic effects of peptide vaccines (16–19).

Peptide amphiphile micelles (PAMs) have emerged as a promising vaccine carrier capable of inducing strong and durable prophylactic antibody responses (20,21). Our recent work has uncovered that certain physical properties of PAM vaccines including size and charge greatly influence their efficacy. Specifically, spherical and short cylindrical PAMs tens of nanometers in

Theme Editor: Ho-Leung Fung

Electronic supplementary material The online version of this article (https://doi.org/10.1208/s12248-018-0233-6) contains supplementary material, which is available to authorized users.

[1] Department of Chemical Engineering, University of Missouri, W2027 Lafferre Hall, 416 S. 6th Street, Columbia, Missouri 65211, USA.
[2] Department of Biochemistry, University of Missouri, Columbia, Missouri 65211, USA.
[3] Department of Bioengineering, University of Missouri, Columbia, Missouri 65211, USA.
[4] Molecular interactions Core, University of Missouri, Columbia, Missouri 65211, USA.
[5] To whom correspondence should be addressed. (e–mail: uleryb@missouri.edu)

size with near neutral surface charge were found to best enhance antigen immunogenicity (22,23). While promising, PAMs alone may not induce strong enough host immune responses to be protective. Therefore, co-delivering molecular adjuvants, compounds with known immunostimulatory behavior, with antigen-based PAMs has the potential to yield a novel synthetic vaccine formulation with potent bioactivity. To test this theory, this paper focuses on creating and evaluating PAMs comprised of the model antigen OVA_{BT}-$(KE)_4$ and the toll-like receptor 2 (TLR-2) agonist 2,3-dipalmitoyl-S-glyceryl cysteine (Pam_2C) as these molecules have shown potent antigenicity and adjuvanticity, respectively (21–26). From these efforts, new design rules which can be leveraged for the creation of future disease-specific PAM vaccines will hopefully be determined.

MATERIALS AND METHODS

Peptide and Peptide Amphiphile Synthesis, Purification, and Characterization

OVA_{BT} peptide (ESLKISQAVHAAHAEINEAGRE) with an additional zwitterion-like repeat $(KE)_4$ added to the C terminus (ESLKISQAVHAAHAEINEAGREKEKEKEKE) was synthesized on rink amide resin (Chem-Impex International, SC Wood Dale, IL) by solid-phase synthesis on a multiple peptide synthesizer (Advanced ChemTech 396 Omega, Louisville, KY) using Fmoc chemistry. The N terminus was then either acetylated with acetic anhydride or covalently coupled to 5,6-carboxyfluorescein (FAM, EMD millipore) to cap or fluorescently label the peptide, respectively. OVA_{BT} peptide amphiphile (PA) was synthesized similarly but Fmoc-Lys(Fmoc)-OH was added to the N terminus of OVA_{BT} on resin after which the Fmoc groups were deprotected with 25% piperidine in dimethylformamide (DMF). The two primary amines were then conjugated with palmitic acid (Palm) using a 1:5:4.2:10 Palm:HOBT:HBTU:DIPEA ratio in n-methyl-2-pyrrolidone (NMP). Fluorophore-labeled OVA_{BT} PAs were synthesized similarly except an additional Fmoc-Lys(ivDDE)-OH was positioned between the Fmoc-Lys(Fmoc)-OH and N terminus of the OVA_{BT}-$(KE)_4$ peptide on resin. The ivDDE group was deprotected by 2% hydrazine in DMF allowing for FAM attachment to the primary amine side group. Adjuvant templated OVA_{BT} PAs were synthesized similarly as previously described except Pam_2C instead of Fmoc-Lys(Fmoc)-OH was attached to the N terminus of OVA_{BT} on resin. All peptides and PAs were cleaved from resin and their side groups deprotected by a single reaction consisting of 2 h of exposure to the following mixture: TFA, thioanisole, phenol, water, ethanedithiol, and triisopropylsilane (87.5:2.5:2.5:2.5:2.5). Precipitation and washing with diethyl ether yielded crude products which were characterized and purified by mass spectrometry aided semi-preparative high-pressure liquid chromatography (HPLC, Beckmann Coulter, Fullerton, CA) using a C4 or C18 column (Milford, MA) and in-house solvent gradients. Pam_2C-SK_4 was purchased from InvivoGen (San Diego, CA) and 5(6)-carboxytetramethylrhodamine (TAMRA) modified Pam_2C-SK_4 was synthesized in-house according to the previously mentioned solid-phase synthesis technique with TAMRA attached to the N terminus of Pam_2C-SK_4 while the PA is still on resin. Similar to our previous work, micelle formation, morphology, size, and secondary structure were assessed by critical micelle concentration (CMC), transmission electron microscopy (TEM), dynamic light scattering (DLS), and circular dichroism (CD), respectively (22,23). Förster resonance energy transfer (FRET) was conducted similarly to a previously described protocol (24). In brief, 10% adjuvant supplemented peptide was formulated by directly mixing product solutions yielding 36 μM 2.1% FAM-labeled OVA_{BT} peptide with 4 μM TAMRA-labeled Pam_2C-SK_4. To form 10% adjuvant associated PAMs, methanol solubilized, air dried, and rehydrated mixture yielding 36 μM 2.1% FAM-labeled OVA_{BT} with 4 μM TAMRA-labeled Pam_2C-SK_4 heterogeneous PAMs. Single fluorophore-labeled monomers at the same concentrations (i.e., 0.756 μM for FAM or 4 μM for TAMRA) were included as controls. Fluorescence spectra were collected using a Cytation 5 fluorospectrophotometer for which laser excitation was set at 450 nm and emitted light was collected from 475 to 700 nm.

Vaccine Fabrication

Vaccine formulations used for *in vitro* and *in vivo* experiments included antigen and/or adjuvant and are shown in Scheme 1 and were fabricated by a few different methods. In specific, 10% adjuvant supplemented peptide and 10% adjuvant associated PAMs were prepared similarly to previously described methods (21,24). Briefly, 90% molar ratio OVA_{BT} peptide and 10% molar ratio Pam_2C-SK_4 were mixed directly in phosphate buffered saline (PBS) to form 10% adjuvant supplemented peptide. By contrast, to form 10% adjuvant associated PAMs, 90% molar ratio $Palm_2K$-OVA_{BT}-$(KE)_4$ and 10% molar ratio Pam_2C-SK_4 adjuvant were first dissolved in methanol to produce a heterogeneous mixture and air dried to form a thin film before being rehydrated in PBS. Thus, we expect segregation of antigen and adjuvant for 10% adjuvant supplemented peptide compared to co-localization with the 10% adjuvant associated PAMs which is supported by both Fig. S1 and previous studies (24). To form 10% adjuvant templated PAMs, 90% molar ratio $Palm_2K$-OVA_{BT}-$(KE)_4$ and 10% molar ratio Pam_2C-OVA_{BT}-$(KE)_4$ were co-assembled into the same micelles using similar methanol-dry method. All other groups (i.e., Peptide, PAMs, 100% adjuvant templated PAs, Pam_2C-SK_4, and Pam_2C-OVA_{BT}-KE_4) were made by simply dissolving products in aqueous solution.

Preparation and Activation of Bone Marrow-Derived Dendritic Cells

Balb/c mouse femurs and tibias were harvested from which cells were collected by flushing the bone marrow with complete RPMI 1640 media that was passed through a cell strainer (70 μM mesh size). Red blood cells were lysed by ammonium-chloride-potassium (ACK) lysis buffer before stromal cells were seeded on non-tissue culture treated petri-dishes. The cells were cultured in bone marrow-derived dendritic cells (BMDC) differentiation media (RPMI 1640 supplemented with 10% fetal bovine serum (FBS), 1% penicillin-streptomycin, 50 μM β-mercaptoethanol, and 20 ng/mL granulocyte-macrophage colony-stimulating factor (GM-CSF) at 37 °C with 5% CO_2 for which culture media was refreshed on days 3, 6, and 8. Any stromal cells expected to have differentiated into BMDCs should have done so by

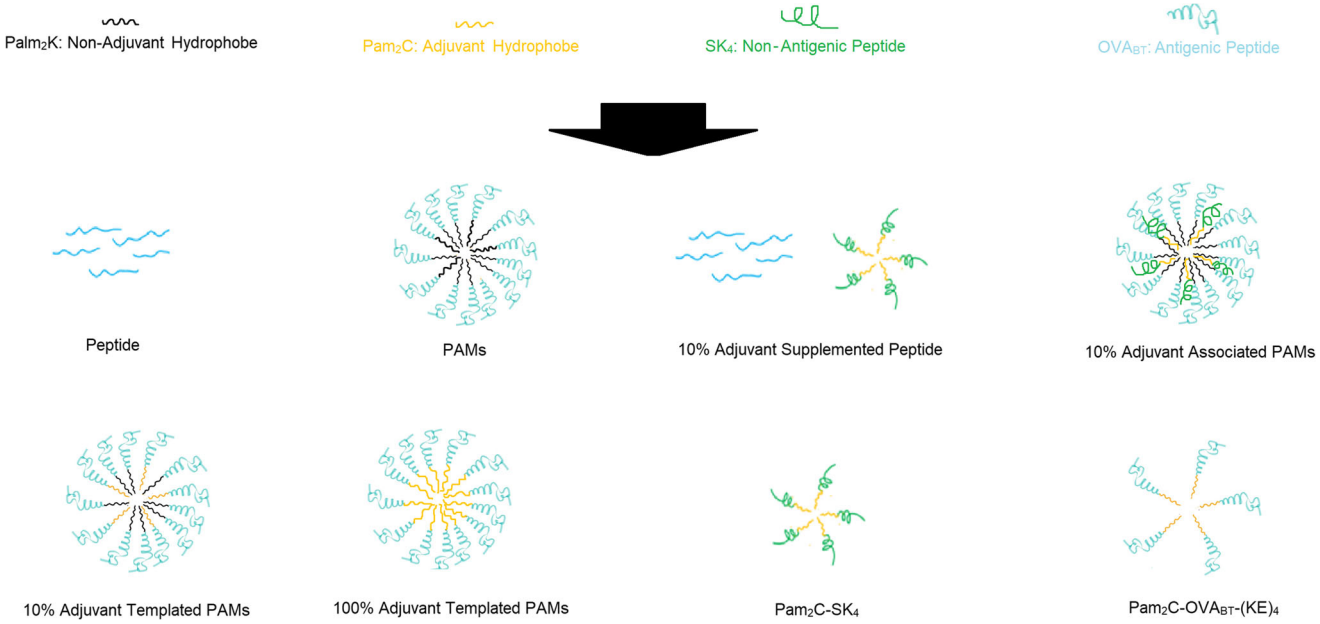

Scheme 1. *In vitro* and *in vivo* vaccine formulations. Combinations were either mixed, solvent cast, or directly hydrated to achieve the different preparations shown

10 days of incubation, so the mixed cell population was purified using mouse CD11c nano beads (Biolegend) at that time point. The isolated BMDCs were seeded in 24-well plates at 2×10^5 cells/well, allowed to incubate overnight, and then exposed to one of a variety of different vaccine formulations (Table I) for 24 h. Vaccine-treated DCs were harvested, blocked with anti-CD16/32 for 10 mins, and then stained with fluorescently-labeled antibodies (i.e., APC-MHC II, FITC-CD40, and PE-CD86—Biolegend) for 30 min. Stained cells were fixed with 4% paraformaldehyde and analyzed via a BD LSRFortessa X-20 flow cytometer.

Murine Vaccination

Sex-matched Balb/C mice (4 males and 4 females per group) 6–8 weeks old were obtained from Jackson Laboratories and subcutaneously administrated different vaccine formulations (Table II) in the nape of the neck. Primary and boost injections were given at week 0 and week 4, respectively. Whole blood was collected from the saphenous vein every other week (i.e., weeks 2, 4, 6, 8, 10, 12, 14, and 16) and centrifuged at 10,000 rpm for 10 min to separate out the red blood cells. The resulting serum supernatant was harvested and stored at −80 °C until further analyzed. This *in vivo* experiment was performed using protocols approved by the Animal Care and Use Committee (ACUC) at the University of Missouri.

Antibody Response Characterization

High binding, 96-well ELISA plates (Santa Cruz Biotechnology) were coated overnight with 4 μg/mL OVA_{BT} peptide in PBS. Wells were washed with PBS-T (0.05% Tween-20 in PBS) and blocked with 10% FBS in PBS (blocking buffer) for 1 h. Serum was serially diluted twofold in blocking buffer across the plate and incubated for 2 h. Wells were then washed with PBS-T and incubated with 1:3000 diluted detection antibody for 1 h. After additional washing with PBS-T, wells were incubated for 30 min with 100 μL TMB substrate (Biolegend) and optical density (OD) was measured at 650 nm absorbance using a Biotek

Table I. Nine Different Vaccine Formulations used for the *In Vitro* BMDC Activation Study

BMDC stimulus groups	DOSE
No stimulus	PBS
Peptide	1.8 μM OVA_{BT}-$(KE)_4$
PAMs	1.8 μM $Palm_2K$-OVA_{BT}-$(KE)_4$
10% adjuvant supplemented peptide	1.8 μM $Palm_2K$-OVA_{BT}-$(KE)_4$ + 0.2 μM Pam_2C-SK_4
10% adjuvant templated PAMs	1.6 μM $Palm_2K$-OVA_{BT}-$(KE)_4$/0.2 μM Pam_2C-OVA_{BT}-$(KE)_4$
100% adjuvant templated PAMs	1.8 μM Pam_2C-OVA_{BT}-$(KE)_4$
Pam_2C-OVABT-$(KE)_4$	0.2 μM Pam_2C-OVA_{BT}-$(KE)_4$
Pam_2C-SK_4	0.2 μM Pam_2C-SK_4

Table II. Four Different Vaccine Formulations Used for the *In Vivo* Immunization Experiment

Vaccination groups	Primary regimen	Boost regimen
10% adjuvant supplemented peptide	200 nmol OVA_{BT}-$(KE)_4$ + 22.2 nmol Pam_2C-SK_4	100 nmol OVA_{BT}-$(KE)_4$ + 11.1 nmol Pam_2C-SK_4
10% adjuvant associated PAMs	200 nmol $Palm_2K$-OVA_{BT}-$(KE)_4$/22.2 nmol Pam_2C-SK_4	100 nmol $Palm_2K$-OVA_{BT}-$(KE)_4$/11.1 nmol Pam_2C-SK_4
10% adjuvant templated PAMs	177.8 nmol $Palm_2K$-OVA_{BT}-$(KE)_4$/22.2 nmol Pam_2C-OVA_{BT}-$(KE)_4$	88.9 nmol $Palm_2K$-OVA_{BT}-$(KE)_4$/11.1 nmol Pam_2C-SK_4
100% Adjuvant Templated PAMs	200 nmol Pam_2C-OVA_{BT}-$(KE)_4$	100 nmol Pam_2C-OVA_{BT}-$(KE)_4$

Boost vaccinations consisting of half the primary dose were given 4 weeks after the primary vaccination

Cytation 5 spectrofluorometer. End-point antibody titers were defined as the greatest serum dilution where ELISA OD was at least twice that of serum from mice vaccinated with PBS. If end-point titers were not reached with one plate, then additional titrations were utilized until ODs were diluted below detection.

Lymphocyte Isolation, Antigenic Challenge, and Stimulus Assessment

Mice were sacrificed 16-week post-primary vaccination after which draining lymph nodes and spleens from immunized mice were collected and grinded with a cell strainer pestle. Spleen cells were further treated with ACK lysis buffer in order to remove red blood cells. Single-cell suspensions of lymph node cells or ACK lysis buffer treated spleen cells were further prepared by filtering through a 70-μm nylon mesh cell strainer. Cells were plated in 96-well tissue culture treated plates at 1.7×10^5 cells/well and stimulated with 25 μg/mL OVA_{BT} peptide. After 72 h of incubation, cell culture supernatants were collected and stored at −80 °C until further analyzed. Cell culture supernatants of pooled samples were screened by a multiplex cytokine kit (Biolegend) to determine any cytokine differences among the vaccination groups. Based on this screening, individual samples were analyzed for their IL-2, IFN-γ, and TNF-α concentrations by cytokine-specific ELISA kits (Biolegend).

Statistical Analysis

JMP software (SAS Institute) was used to make comparisons between groups where an analysis of variance (ANOVA) was performed followed by Tukey's HSD testing to determine pairwise statistically significant differences ($p \leq 0.05$).

RESULTS

Intrinsic Non-immunostimulatory Behavior of PAMs

The bacterial cell wall, particularly its hydrophobic lipid constituents, can act as pathogen molecular associated patterns that stimulate antigen presenting cells (APCs) via cell surface associated molecules like toll-like receptors (TLRs) (27,28). Interestingly, previous research has demonstrated that PAMs do not activate the TLR-2 receptor (21) even when templated with a lipid (i.e., diC_{16}–1′,3′-dihexadecyl N-succinyl-L-glutamate) that is chemically quite similar to the known TLR-2 agonist Pam_2C (29). To expand upon this previous research, the capacity for PAMs to more broadly activate APCs was explored. BMDCs were cultured with either no stimulus, OVA_{BT} peptide, or OVA_{BT} PAMs after which three different cell surface markers associated with cell activation (i.e., MHC II, CD40, and CD86) were evaluated (Fig. 1). No statistically significant differences were observed among any of the treatments utilized.

Antigen|Adjuvant Co-localization Affects PAM Immunogenicity

Without underlying immunostimulatory effects, PAM immunogenicity can be readily enhanced through the co-delivery of known molecular adjuvants. While this could be accomplished by simply mixing PAM and molecular adjuvants immediately before immunization, recent research has demonstrated that direct antigen|adjuvant co-localization can greatly improve vaccine efficacy (17,30–37). Specifically, Pam_2C has been shown to be able to co-localized with antigens via different methods including through hydrophobic association (24) or chemical conjugation (38–40). Though both strategies have shown promising outcomes, their differential impact on antigen immunogenicity has yet to be determined leaving open the question of which one is the optimal antigen/Pam_2C co-localization strategy.

Prior study of PAM vaccines has shown that co-localizing Pam_2C via hydrophobic association greatly increased host antibody titer production (24). Also, as Pam_2C is quite hydrophobic and possesses a similar chemical structure to $Palm_2K$ (Scheme S1), it was hypothesized that it could be utilized to directly template PAMs. The PA Pam_2C-OVA_{BT}-$(KE)_4$ was synthesized and found to readily form spherical and short cylindrical micelles in water analagous to $Palm_2K$-OVA_{BT}-$(KE)_4$ (Fig. S2) (22,23). To probe how antigen|adjuvant co-localization can impact antibody responses, mice were immunized subcutaneously in the nape of the neck with the formulations outlined in Table II. OVA_{BT}-specific IgG antibody was evaluated by ELISA using serum collected every other week (Fig. 2). All four vaccine formulations induced total IgG that peaked at 2-week post-boost immunization (i.e., week 6) and slowly decreased thereafter for the rest of the study. The results indicate that 10% adjuvant associated PAMs induced significantly higher total IgG titers than mice vaccinated with 10% adjuvant supplemented peptide at all post-vaccination time points. This agrees with previous studies using a group A Streptococcus antigen (21,24).

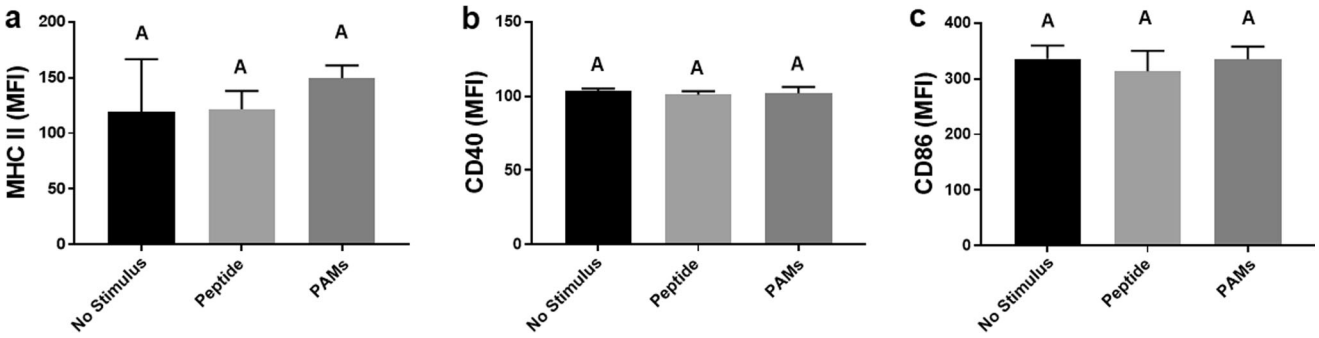

Fig. 1. PAMs are not inherently immunostimulatory. BMDCs were stimulated with peptide or PAMs for 24 h for which no stimulus was utilized as a negative control. Cell activation was assessed by determining the quantity of **a** MHC II, **b** CD40, and **c** CD86 present on the cell surface. Neither exposure to peptide nor PAMs was found to activate any of these known BMDC activation markers above background levels. Within a graph, groups that possess different letters have statistically significant differences in mean ($p \leq 0.05$) whereas those that possess the same letter are similar ($p > 0.05$)

Antigen|adjuvant co-localization was further explored by comparing the efficacy of two different co-localization methodologies (i.e., adjuvant associated–hydrophobic driving force; adjuvant templated–covalent coupling). The data shows that 10% adjuvant templated PAMs induced significantly lower antibody titer IgG than 10% adjuvant associated PAMs at most time points post-boost vaccination (i.e., weeks 6, 10, 12, and 14). Even when the Pam_2C adjuvant dose was increased by ninefold (i.e., 100% adjuvant templated PAMs), no improvement in antibody production was observed. IgG subtypes (i.e., IgG1, IgG2a, and IgG3) were similarly evaluated 2-week post-boost vaccination (i.e., week 6) (Fig. S2). Interestingly, IgG1 and IgG3 showed a similar trend as total IgG. For IgG2a, 10% adjuvant templated PAMs induced no detectable antibody production indicating that different co-localization strategies can alter antibody subtype polarization.

Antigen|Adjuvant Co-localization Influences Cellular Responses

In addition to antibody production, Pam_2C is known to exert strong cell stimulatory effects (41–45). To assess cellular responses induced by different vaccine formulations, murine spleens and lymph nodes were collected 16 weeks after primary vaccination, homogenized into single-cell suspensions, and stimulated with OVA_{BT} peptide. Cell culture medium was collected 72 h after re-stimulation and IL-2, IFN-γ, and TNF-α were measured from both stimulated spleen cells (Fig. 3a–c) and lymph node cells (Fig. 3d–f). Both spleen cells and lymph node cells responded similarly to antigen exposure with 10% adjuvant associated PAMs inducing the most potent cytokine production. A couple of mice vaccinated with 100% adjuvant templated PAMs induced appreciable cytokine production but none of these

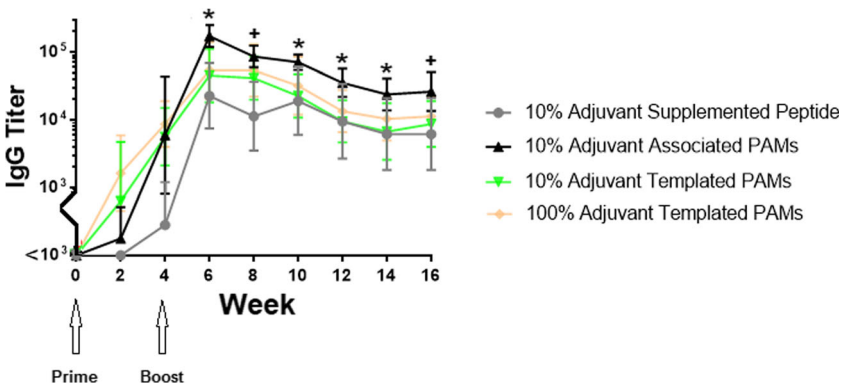

Fig. 2. Antigen|adjuvant co-localization strategy affects antibody production kinetics. Mice were immunized by a prime/boost regimen with one of four vaccine formulations. Serum was collected every other week from which total IgG serum titers were evaluated by ELISA. Antibody production kinetics showed a similar trend regardless of vaccine formulation with titers peaking 2 week post-boost immunization (i.e., week 6) and slowly decreasing thereafter with sustained titers still present 12-week post-boost immunization (i.e., week 16). Statistically significantly higher IgG titers were seen with hydrophobically associated antigen/adjuvant (i.e., 10% adjuvant associated PAMs) compared to antigen and adjuvant segregated from each other (i.e., 10% adjuvant supplemented peptide) or chemically tethered together (i.e., 10% adjuvant templated PAMs or 100% adjuvant templated PAMs). *10% adjuvant associated PAMs possessed statistically significant differences in mean ($p \leq 0.05$) than the other three groups assessed at the same time points; $^{+}$10% adjuvant associated PAMs induced significantly differences in mean ($p \leq 0.05$) than 10% adjuvant supplemented peptide

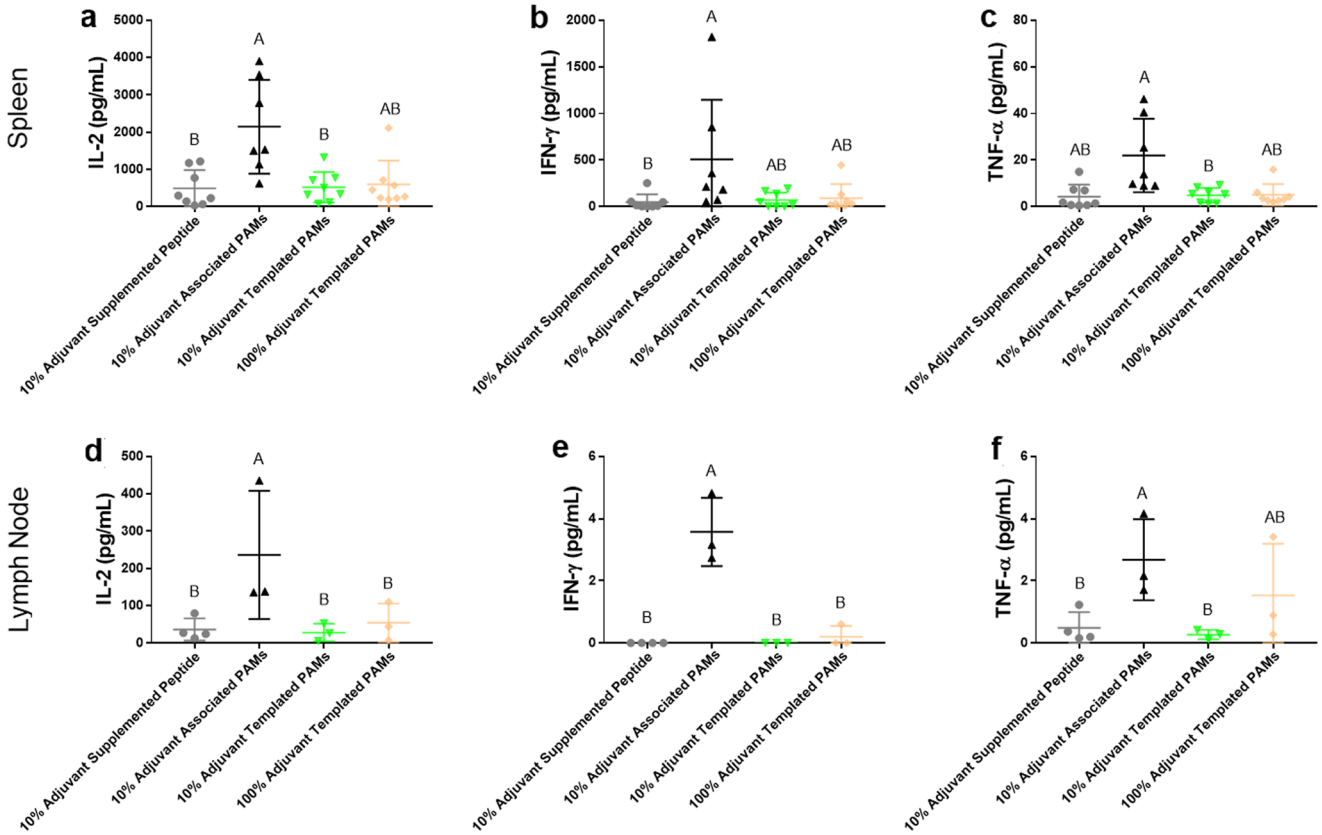

Fig. 3. Different antigen|adjuvant co-localization strategies affect cellular responses. **a–c** Cell culture supernatants collected from OVA_{BT} peptide challenged spleen cells 72 h after re-stimulation with OVA_{BT} peptide were analyzed for their cytokine content (i.e., IL-2, IFN-γ, and TNF-α) by ELISA. **d–f** OVA_{BT} challenged lymph node cell culture supernatants were similarly collected 72 h after OVA_{BT} peptide re-stimulation and the same cytokines (i.e., IL-2, IFN-γ, and TNF-α) were evaluated. Both spleen cells and lymph node cells showed a similar trend where only 10% adjuvant associated PAMs induced appreciable cytokine production over 10% adjuvant supplemented peptide. Within a graph, groups that possess different letters have statistically significant differences in mean ($p \leq 0.05$) whereas those that possess the same letter are statistically similar ($p > 0.05$)

results were statistically significant above 10% adjuvant supplemented peptide.

Antigen|Adjuvant Co-localization Strategies Affect Pam_2C Adjuvanticity

To better probe why different antigen|adjuvant co-localization methods resulted in varying vaccine immunogenicity, a more in-depth *in vitro* analysis was conducted. One of the major differences in the four vaccine formulations used was whether Pam_2C was tether to SK_4 (10% adjuvant supplemented peptide and 10% adjuvant associated PAMs) or OVA_{BT} (10% or 100% adjuvant templated PAMs) (Fig. 4a and Fig. S3a). BMDCs were cultured with one of the four vaccine formulations for 24 h after which three different cell surface markers associated with cell activation (i.e., MHC II, CD40, and CD86) were evaluated (Fig. 4b–d). Experimental groups that included Pam_2C-SK_4 induced significantly higher CD86 and MHC II expression on BMDCs compared to groups that included Pam_2C-OVA_{BT}-$(KE)_4$. This difference was consistent with cell surface marker analysis conducted for BMDCs exposed to only Pam_2C-SK_4 or Pam_2C-OVA_{BT}-$(EK)_4$ (Fig. S3b-d).

DISCUSSION

Though PAMs have shown tremendous promise as self-adjuvanting vaccine delivery vehicles (21,24,46), there is still much to be learned about which aspects of their design influence their immunogenicity. Our recent efforts have shown that PAM size and charge can be readily altered and this directly enhances or suppresses host immune responses to incorporated peptide antigen (22,23). Specifically, the most potent PAM formulation (i.e., $Palm_2K$-OVA_{BT}-$(KE)_4$) was found to possess the greatest capacity to cross multiple biological barriers including trafficking to the draining lymph nodes and being uptaken by APCs. While exciting, it is unknown whether PAMs possess any intrinsic immunostimulatory properties. Previous research has demonstrated that PAMs do not directly stimulate TLR-2 receptors (21). Though interesting, other potential pathways (e.g., other TLRs, NOD-like receptors, and RIG-like receptors) could be activated by PAMs. In order to evaluate the immunostimulatory capacity of PAMs, their capacity to generally activate APCs was explored. Remarkably, PAMs alone failed to significantly stimulate BMDCs compared to the potent response seen with a known molecular adjuvant (i.e., Pam_2C) as evidenced by a lack of cell surface co-

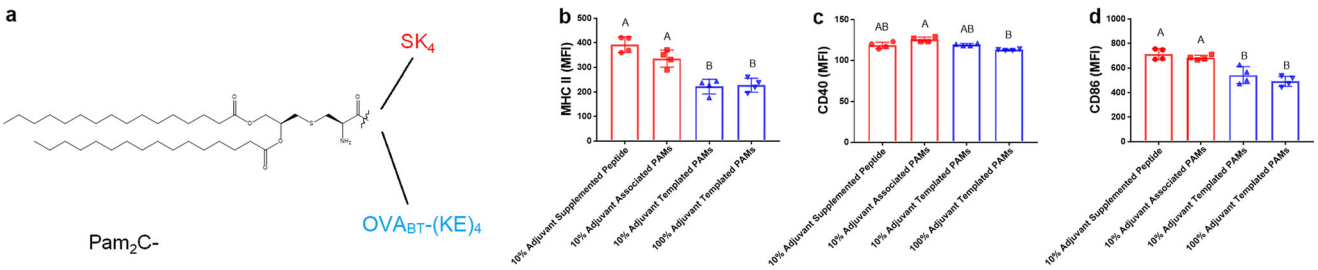

Fig. 4. Different peptide sequences influence Pam_2C adjuvanticity. **a** The scheme shows that Pam_2C was tethered with one of two peptide sequences, SK_4 or OVA_{BT}-$(KE)_4$. **b–d** BMDCs were stimulated with one of four vaccine formulations for 24 h before the activation associated surface markers **b** MHC II, **c** CD40, and **d** CD86 were stained and assessed by flow cytometry. Vaccine groups possessing Pam_2C coupled to SK_4 were found to exert strong immunostimulatory effects than those with Pam_2C bound to OVA_{BT}-$(KE)_4$. Within a graph, groups that possess different letters have statistically significant differences in mean ($p \leq 0.05$) whereas those that possess the same letter are statistically similar ($p > 0.05$)

stimulatory marker expression changes (Figs. 1 and 4). Therefore, previously reported PAM immunogenicity appears to be a more related to its targeted delivery capacity (22) instead of an innate ability to activate APCs.

The lack of intrinsic immunostimulatory capacity allows for PAM vaccine immunogenicity to be enhanced through the incorporation of molecular adjuvants. Previously, the hydrophobic association of Pam_2C-SK_4 with PAMs at a 90/10 antigen/adjuvant molecular ratio was found to significantly enhance immunogenicity over adjuvant supplemented peptide and PAMs alone for group A Streptococcus peptide antigen (24). When a similar formulation was utilized in this work (i.e., 10% adjuvant associated PAMs), comparable improvements in antigen-specific antibody induction and isotype production were observed (Fig. 2 and Fig. S2). Cellular responses complemented these results as lymph nodes and spleens from mice vaccinated with 10% adjuvant associated PAMs possessed lymphocytes capable of producing a desirable cytokine profile in response to antigen restimulation (Fig. 3). Taken together, these results support the concept that adjuvant/antigen co-localization using PAM vaccines can be a powerful approach for improving subunit vaccination.

Although exciting, hydrophobic association is not the only method available for achieving adjuvant incorporation. Covalent coupling antigens to Pam_2C have been previously shown to enhance peptide immunogenicity (40,47) and the chemical similarities between Pam_2K and Pam_2C potentially allow for direct adjuvant micelle templating. The results support this idea as Pam_2C-OVA_{BT}-$(KE)_4$ readily self-assembled in water at a low CMC (0.32 μM—Fig. S2a) into spherical and short cylindrical micelles (Fig. S2b) presenting peptide mostly in the β sheet conformation (95.0%—Fig. S2c). These micellar factors are very similar to those previously identified for $Palm_2K$-OVA_{BT}-$(KE)_4$ (e.g., 0.20 μM CMC and 91.4% β sheet content) eliminating some potentially confounding variables between the formulations (23). Interestingly, adjuvant coupling yielded a vaccine formulation (i.e., 10% adjuvant templated PAMs) with a weakened capacity to induce OVA_{BT}-specific antibody production (Fig. 2 and Fig. S3) and antigen sensitive lymphocytes (Fig. 3) compared to 10% adjuvant associated PAMs. This limitation was not even able to be overcome by increasing adjuvant content ninefold through the use of only antigen-adjuvant PAs (i.e., 100% adjuvant templated PAMs). The vaccination response with both adjuvant templated PAM formulations was found to actually be quite similar to 10% adjuvant supplemented peptide.

The diminished immunogenicity caused by antigen-adjuvant coupling, especially when a greater quantity of adjuvant was used, was a quite surprising result. In order to further investigate why different co-localization strategies so greatly impacted immunogenicity, additional APC activation studies were conducted. The results revealed that both adjuvant templated PAM formulations induced less MHC II and CD86 surface marker expression on BMDCs compared to cells exposed to 10% adjuvant supplemented peptide and 10% adjuvant associated PAMs (Fig. 4b, d). The fundamental difference in these formulations is which peptide is tethered to Pam_2C. Additional *in vitro* BMDC stimulation assessment using just Pam_2C-SK_4 and Pam_2C-OVA_{BT}-$(KE)_4$ (Fig. S4b, d) support these results, indicating the peptidic component of the Pam_2C amphiphile influences its immunogenicity. Although PAM vaccine size has been shown to play an important role in influencing the host antibody response (22), immunogenicity differences observed for adjuvant associated PAMs and adjuvant templated PAMs were likely due to adjuvant incorporation method as they were found to be similar in size (Table S1).

The diminished or lack of immunostimulatory behavior seen with another formulation (i.e., adjuvant templated PAMs) likely stems from the requirement for proper TLR2 receptor-agonist binding. Protein crystallography has revealed that the lipid binding pocket in TLR2 and agonist association with TLR6 dictates receptor activation is dependent on a few key chemical features (48). Though $Palm_2K$, as well as the previously utilized diC_{16}, possess considerable similarities to the known TLR2 agonist Pam_2C, their slight differences are quite important when it comes to stimulating the TLR2 receptor. The hydrophobic binding cleft of TLR2 is specifically designed for palmitoyl moieties that are separated by two hydrocarbons (48). While Pam_2C satisfies this requirement, $Palm_2K$ possesses a four hydrocarbon spacer. This additional length alters the protein residue pocket alignment which is necessary to stabilize the lipid yielding diminished binding capacity similar to what has been shown with stearic acid modified glycerylcysteine (49). The presence of the thioether in Pam_2C is also important as it has been shown to bind multiple residues in TLR2 as well as a residue in TLR6 helping to stabilize protein dimerization

(48). The replacement of this with an ether significantly diminishes binding (50). Additionally, palmitoyl binding chemistry plays an important role in agonist-protein binding. While the replacement of one ester with an amide only partially inhibits agonist binding, replacing both groups, like what is done with Pam_2K, completely prevents association (50). Therefore, the lack of APC activation by $Paml_2K$ is likely due to its inability to function as a TLR2 agonist.

The reduced immunostimulatory behavior found when Pam_2C is bound to OVA_{BT}-$(KE)_4$ instead of SK_4 is probably caused by similar binding changes. Though the hydrophobic moiety is the same in this case, research has shown that agonist peptide sequence plays an important role in TLR2 activation as well (51,52). The presence of tetralysine has been shown to enhance binding fivefold (50), so its absence likely will at least somewhat diminish Pam_2C bioactivity. More impactful though is the presence of the N-terminal serine which has been shown to undergo hydrogen bonding with a carbonyl group in the protein backbone of TLR2 (48). The lack of this group has been shown to diminish binding four to five orders of magnitude (50). The N-terminal glutamic acid of OVA_{BT}-$(KE)_4$ is too long to facilitate this necessary hydrogen bonding likely greatly impacting its adjuvanticity. In addition, directly linking the antigen and the adjuvant may diminish their respective effects. Recent research has shown that decoupling antigen and adjuvant can actually maintain or improve vaccine immunogenicity (53,54). One rationale behind this theory is that antigens and adjuvants carry out their functions in different places in the APC. While TLR agonist adjuvants must interact with their corresponding TLR on the cell surface membrane (55–57) or early endosome (58–60), antigens need to be transported into late endosome or lysosomes and cleaved into small fragments before being presented by MHC II molecules on the cell membrane (61). Covalently tethering antigen and adjuvant together into one PA may require each biomolecule to carry out only a singular function. Therefore, while co-localizing antigen and adjuvant into a single PAM is attractive for delivering both molecules to the same APC, having the capacity to readily dissociate these from one another may allow for each to function optimally.

CONCLUSION

While previous studies have shown that PAMs can be utilized to improve subunit vaccine efficacy (21,22,24), design rules associated that govern this behavior are sorely lacking. This work expands on previous research, revealing that PAM immunogenicity is likely dictated by their targeted trafficking ability (i.e., lymph node accumulation and APC uptake) instead of directly stimulating APCs (e.g., by interactions with toll-like receptors or mannose receptors). PAM immunogenicity can be further enhanced through the co-localization of a molecular adjuvant (i.e., Pam_2C). Interestingly, the method by which the adjuvant is incorporated was found to make an appreciable difference in peptide immunogenicity. Specifically, hydrophobic association was found to enhance both antibody and cellular responses over adjuvant supplemented peptide whereas covalent tethering showed no improvement even when the quantity of adjuvant delivered was greatly increased. Upon further analysis, these results correspond to established molecular features that govern receptor agonist activity. The results reported help inform future adjuvant incorporated PAM formulation design by allowing for better and more rapid optimization of this platform technology for a variety of different types of vaccines. Further studies are in necessary to create a more comprehensive tool box for Pam_2C incorporation including the use of different peptide sequences with modified conditions (e.g., dose sparing, different peptide epitopes, and stability). These together would allow for the establishment of more comprehensive vaccine adjuvant optimization strategies as well as the creation of vaccines designed against a variety of emerging and re-emerging diseases.

ACKNOWLEDGEMENTS

We thank Professor Thomas Phillips, Professor Jeffrey Adamovicz, Alexis Dadelahi, and Dr. Curtis Pritzl for their useful input on this work. We also thank Biolegend technical support team for their assistance on flow cytometry and cytokine multiplex assays.

Funding Information This work is supported by the University of Missouri start-up funding, the University of Missouri research council board, and the PhRMA Foundation.

REFERENCES

1. Fenner F, Henderson DA, Arita I, Jezek Z, Ladnyi ID, Organization WH. Smallpox and its eradication. 1988.
2. Fine PE, Carneiro IA. Transmissibility and persistence of oral polio vaccine viruses: implications for the global poliomyelitis eradication initiative. Am J Epidemiol. 1999;150(10):1001–21.
3. Mast E, Mahoney F, Kane M, Margolis H. Hepatitis B vaccine. Vaccines, 4th ed Philadelphia: WB Saunders Company 2004:299–338.
4. Babiuk LA. Broadening the approaches to developing more effective vaccines. Vaccine. 1999;17(13):1587–95.
5. Brown F. Peptide vaccines: fantasy or reality? World J Microbiol Biotechnol. 1992;8:52–3.
6. Levine MM, Sztein MB. Vaccine development strategies for improving immunization: the role of modern immunology. Nat Immunol. 2004;5(5):460–4.
7. Zhang R, Ulery BD. Synthetic vaccine characterization and design. J Bionanosci. 2018;12(1):1–11.
8. Chang TZ, Stadmiller SS, Staskevicius E, Champion JA. Effects of ovalbumin protein nanoparticle vaccine size and coating on dendritic cell processing. Biomater Sci. 2017;5(2):223–33.
9. Deng L, Mohan T, Chang TZ, Gonzalez GX, Wang Y, Kwon Y-M, et al. Double-layered protein nanoparticles induce broad protection against divergent influenza a viruses. Nat Commun. 2018;9(1):359.
10. Acharya AP, Clare-Salzler MJ, Keselowsky BG. A high-throughput microparticle microarray platform for dendritic cell-targeting vaccines. Biomaterials. 2009;30(25):4168–77.
11. Wang L, Chang TZ, He Y, Kim JR, Wang S, Mohan T, et al. Coated protein nanoclusters from influenza H7N9 HA are highly immunogenic and induce robust protective immunity. Nanomedicine. 2017;13(1):253–62.
12. Ross K, Adams J, Loyd H, Ahmed S, Sambol A, Broderick S, et al. Combination nanovaccine demonstrates synergistic enhancement in efficacy against influenza. ACS Biomater Sci Eng. 2016;2(3):368–74.
13. Ross KA, Loyd H, Wu W, Huntimer L, Ahmed S, Sambol A, *et al.* Polyanhydride-based H5 hemagglutinin influenza

nanovaccines elicit protective virus neutralizing titers and cell-mediated immunity. Synthetic nanoparticle-based vaccines against respiratory pathogens 2013:149.
14. An M, Liu H. Dissolving microneedle arrays for transdermal delivery of amphiphilic vaccines. Small. 2017;13(26)
15. Hanson MC, Abraham W, Crespo MP, Chen SH, Liu H, Szeto GL, et al. Liposomal vaccines incorporating molecular adjuvants and intrastructural T-cell help promote the immunogenicity of HIV membrane-proximal external region peptides. Vaccine. 2015;33(7):861–8.
16. Ulery BD, Kumar D, Ramer-Tait AE, Metzger DW, Wannemuehler MJ, Narasimhan B. Design of a protective single-dose intranasal nanoparticle-based vaccine platform for respiratory infectious diseases. PLoS One. 2011;6(3):e17642.
17. Moon JJ, Suh H, Bershteyn A, Stephan MT, Liu H, Huang B, et al. Interbilayer-crosslinked multilamellar vesicles as synthetic vaccines for potent humoral and cellular immune responses. Nat Mater. 2011;10(3):243–51.
18. Zhang P, Chiu Y-C, Tostanoski LH, Jewell CM. Polyelectrolyte multilayers assembled entirely from immune signals on gold nanoparticle templates promote antigen-specific T cell response. ACS Nano. 2015;9(6):6465–77.
19. Tsoras AN, Champion JA. Cross-linked peptide nanoclusters for delivery of oncofetal antigen as a cancer vaccine. Bioconjug Chem. 2018;29:776–85.
20. Barrett JC, Ulery BD, Trent A, Liang S, David NA, Tirrell MV. Modular peptide Amphiphile micelles improving an antibody-mediated immune response to group A Streptococcus. ACS Biomater Sci Eng. 2016;
21. Trent A, Ulery BD, Black MJ, Barrett JC, Liang S, Kostenko Y, et al. Peptide amphiphile micelles self-adjuvant group A streptococcal vaccination. AAPS J. 2015;17(2):380–8.
22. Zhang R, Smith JD, Kramer Jake S, Allen BN, Martin S, Ulery BD. Peptide amphiphile micelle vaccine size and charge influences immunogenicity. ACS Biomater Sci Eng 2018;Submitted.
23. Zhang R, Morton LD, Smith JD, Gallazzi F, White TA, Ulery BD. Instructive design of tri-block peptide amphiphiles for structurally complex micelle formation. ACS Biomater Sci Eng 2018;Accepted.
24. Barrett JC, Ulery BD, Trent A, Liang S, David NA, Tirrell M. Modular peptide amphiphile micelles improve an antibody-mediated immune response to group A Streptococcus. ACS Biomater Sci Eng. 2016;3(2):144–52.
25. Sun T, Han H, Hudalla GA, Wen Y, Pompano RR, Collier JH. Thermal stability of self-assembled peptide vaccine materials. Acta Biomater. 2016;30:62–71.
26. Chen J, Pompano RR, Santiago FW, Maillat L, Sciammas R, Sun T, et al. The use of self-adjuvanting nanofiber vaccines to elicit high-affinity B cell responses to peptide antigens without inflammation. Biomaterials. 2013;34(34):8776–85.
27. Takeuchi O, Hoshino K, Kawai T, Sanjo H, Takada H, Ogawa T, et al. Differential roles of TLR2 and TLR4 in recognition of gram-negative and gram-positive bacterial cell wall components. Immunity. 1999;11(4):443–51.
28. Takeuchi O, Takeda K, Hoshino K, Adachi O, Ogawa T, Akira S. Cellular responses to bacterial cell wall components are mediated through MyD88-dependent signaling cascades. Int Immunol. 2000;12(1):113–7.
29. Basto AP, Leitão A. Targeting TLR2 for vaccine development. J Immunol Res. 2014;2014:1–22.
30. Chiu Y-C, Gammon JM, Andorko JI, Tostanoski LH, Jewell CM. Modular vaccine design using carrier-free capsules assembled from polyionic immune signals. ACS Biomater Sci Eng. 2015;1(12):1200–5.
31. Kuai R, Ochyl LJ, Bahjat KS, Schwendeman A, Moon JJ. Designer vaccine nanodiscs for personalized cancer immunotherapy. Nat Mater. 2016;
32. de Jong S, Chikh G, Sekirov L, Raney S, Semple S, Klimuk S, et al. Encapsulation in liposomal nanoparticles enhances the immunostimulatory, adjuvant and anti-tumor activity of subcutaneously administered CpG ODN. Cancer Immunol Immunother. 2007;56(8):1251–64.
33. Joshi VB, Geary SM, Salem AK. Biodegradable particles as vaccine delivery systems: size matters. AAPS J. 2013;15(1):85–94.
34. Keselowsky BG, Xia CQ, Clare-Salzler M. Multifunctional dendritic cell-targeting polymeric microparticles: engineering new vaccines for type 1 diabetes. Human Vaccines. 2011;7(1):37–44.
35. Sevimli S, Knight FC, Gilchuk P, Joyce S, Wilson JT. Fatty acid-mimetic micelles for dual delivery of antigens and Imidazoquinoline adjuvants. ACS Biomater Sci Eng. 2016;3(2):179–94.
36. Hudalla GA, Modica JA, Tian YF, Rudra JS, Chong AS, Sun T, et al. A self-adjuvanting supramolecular vaccine carrying a folded protein antigen. Adv Healthc Mater. 2013;2(8):1114–9.
37. An M, Li M, Xi J, Liu H. Silica nanoparticle as a lymph node targeting platform for vaccine delivery. ACS Appl Mater Interfaces. 2017;9(28):23466–75.
38. Zom GG, Khan S, Britten CM, Sommandas V, Camps MG, Loof NM, et al. Efficient induction of antitumor immunity by synthetic toll-like receptor ligand–peptide conjugates. Cancer Immunol Res. 2014;2(8):756–64.
39. Denton AE, Wesselingh R, Gras S, Guillonneau C, Olson MR, Mintern JD, et al. Affinity thresholds for naive CD8+ CTL activation by peptides and engineered influenza A viruses. J Immunol. 2011;187(11):5733–44.
40. Moyle PM, Dai W, Zhang Y, Batzloff MR, Good MF, Toth I. Site-specific incorporation of three toll-like receptor 2 targeting adjuvants into semisynthetic, molecularly defined nanoparticles: application to group a streptococcal vaccines. Bioconjug Chem. 2014;25(5):965–78.
41. Shime H, Maruyama A, Yoshida S, Takeda Y, Matsumoto M, Seya T. Toll-like receptor 2 ligand and interferon-γ suppress anti-tumor T cell responses by enhancing the immunosuppressive activity of monocytic myeloid-derived suppressor cells. Oncoimmunology. 2018;7(1):e1373231.
42. Dietrich N, Lienenklaus S, Weiss S, Gekara NO. Murine toll-like receptor 2 activation induces type I interferon responses from endolysosomal compartments. PLoS One. 2010;5(4):e10250.
43. Dowling JK, Dellacasagrande J. Toll-like receptors: ligands, cell-based models, and readouts for receptor action. Toll-Like Receptors: Springer. 2016:3–27.
44. Kulsantiwong P, Pudla M, Srisaowakarn C, Boondit J, Utaisincharoen P. Pam2CSK4 and Pam3CSK4 induce iNOS expression via TBK1 and MyD88 molecules in mouse macrophage cell line RAW264. 7. Inflamm Res. 2017;66(10):843–53.
45. Natarajan M, Lin K-M, Hsueh RC, Sternweis PC, Ranganathan R. A global analysis of cross-talk in a mammalian cellular signalling network. Nat Cell Biol. 2006;8(6):571–80.
46. Black M, Trent A, Kostenko Y, Lee JS, Olive C, Tirrell M. Self-assembled peptide amphiphile micelles containing a cytotoxic T-cell epitope promote a protective immune response in vivo. Adv Mater. 2012;24(28):3845–9.
47. Fagan V, Hussein WM, Su M, Giddam AK, Batzloff MR, Good MF, et al. Synthesis, characterization and immunological evaluation of self-adjuvanting group A Streptococcal vaccine candidates bearing various lipidic adjuvanting moieties. Chembiochem. 2017;18(6):545–53.
48. Kang JY, Nan X, Jin MS, Youn S-J, Ryu YH, Mah S, et al. Recognition of lipopeptide patterns by toll-like receptor 2-toll-like receptor 6 heterodimer. Immunity. 2009;31(6):873–84.
49. Agnihotri G, Crall BM, Lewis TC, Day TP, Balakrishna R, Warshakoon HJ, et al. Structure–activity relationships in toll-like receptor 2-agonists leading to simplified monoacyl lipopeptides. J Med Chem. 2011;54(23):8148–60.
50. Wu W, Li R, Malladi SS, Warshakoon HJ, Kimbrell MR, Amolins MW, et al. Structure− activity relationships in toll-like receptor-2 agonistic diacylthioglycerol lipopeptides. J Med Chem. 2010;53(8):3198–213.
51. Azuma M, Sawahata R, Akao Y, Ebihara T, Yamazaki S, Matsumoto M, et al. The peptide sequence of diacyl lipopeptides determines dendritic cell TLR2-mediated NK activation. PLoS One. 2010;5(9):e12550.
52. Fujimoto Y, Hashimoto M, Furuyashiki M, Katsumoto M, Seya T, Suda Y, et al. Lipopeptides from Staphylococcus aureus as Tlr2 ligands: prediction with mrna expression, chemical synthesis, and immunostimulatory activities. Chembiochem. 2009;10(14):2311–5.

53. Kasturi SP, Skountzou I, Albrecht RA, Koutsonanos D, Hua T, Nakaya HI, et al. Programming the magnitude and persistence of antibody responses with innate immunity. Nature. 2011;470(7335):543–7.
54. Mohsen MO, Gomes AC, Cabral-Miranda G, Krueger CC, Leoratti FM, Stein JV, et al. Delivering adjuvants and antigens in separate nanoparticles eliminates the need of physical linkage for effective vaccination. J Control Release. 2017;251:92–100.
55. Nomura F, Akashi S, Sakao Y, Sato S, Kawai T, Matsumoto M, et al. Cutting edge: endotoxin tolerance in mouse peritoneal macrophages correlates with down-regulation of surface toll-like receptor 4 expression. J Immunol. 2000;164(7):3476–9.
56. Akashi S, Saitoh S-i, Wakabayashi Y, Kikuchi T, Takamura N, Nagai Y, et al. Lipopolysaccharide interaction with cell surface toll-like receptor 4-MD-2. J Exp Med. 2003;198(7):1035–42.
57. Triantafilou M, Gamper FG, Haston RM, Mouratis MA, Morath S, Hartung T, et al. Membrane sorting of toll-like receptor (TLR)-2/6 and TLR2/1 heterodimers at the cell surface determines heterotypic associations with CD36 and intracellular targeting. J Biol Chem. 2006;281(41):31002–11.
58. Kužnik A, Benčina M, Švajger U, Jeras M, Rozman B, Jerala R. Mechanism of endosomal TLR inhibition by antimalarial drugs and imidazoquinolines. J Immunol. 2011;186(8):4794–804.
59. Takeshita F, Gursel I, Ishii KJ, Suzuki K, Gursel M, Klinman DM, editors. Signal transduction pathways mediated by the interaction of CpG DNA with toll-like receptor 9. Semin Immunol; 2004: Elsevier.
60. Napolitani G, Rinaldi A, Bertoni F, Sallusto F, Lanzavecchia A. Selected toll-like receptor agonist combinations synergistically trigger a T helper type 1–polarizing program in dendritic cells. Nat Immunol. 2005;6(8):769–76.
61. Neefjes J, Jongsma ML, Paul P, Bakke O. Towards a systems understanding of MHC class I and MHC class II antigen presentation. Nat Rev Immunol. 2011;11(12):823–36.